34th Annual International Conference of the IEEE EMBS
San Diego, California USA, 28 August - 1 September, 2012

Multi-lead QRS Detection Using Window Pairs*

Sami Torbey, Selim G. Akl, and Damian P. Redfearn

***Abstract*—We designed a novel approach for multi-lead QRS detection. The algorithm uses one equation with two different window widths to generate a feature signal and a detection threshold. This enables it to adapt to various changes in QRS morphology and noise levels, resulting in a detection error rate of just 0.29% on the MIT-BIH Arrhythmia Database. The algorithm is also computationally efficient and capable of resolving differences between multiple leads by automatically attaching a confidence value to each QRS detection.**

I. Introduction

The electrocardiogram or ECG is a periodic signal where each period or heartbeat comprises various waves (namely the P, Q, R, S and T-waves) depicting cardiac depolarization and repolarization as seen from one or more leads. The QRS complex represents ventricular depolarization and is usually the most prominent wave in a given heartbeat (due to its rapid rate of change and large amplitude). This makes it very useful as a fiducial point both for detecting other waves as well as for measuring heart rate, rhythm, and related clinical indices such as heart rate variability.

QRS morphology can vary greatly, due to both noise and physiological reasons such as arrhythmias. Potential noise sources include electromyographic (EMG) interference from muscular activity of noncardiac origin, 50 and 60 Hz power line artefact, baseline drift, amplitude modulation due to respiratory rhythms, T-waves with similar frequency and amplitude characteristics, and composite noise arising from a combination of sources.

In this paper, we present and validate a novel multi-lead QRS detection algorithm that is highly resistant to noise artefact while requiring little computational power and no manual input.

II. Algorithm

QRS detection algorithms generally consist of two stages: a pre-processing or feature extraction stage including linear and nonlinear filtering, and a decision stage involving peak annotation and decision logic. In most cases, the decision stage is heuristic and the performance of the algorithm depends heavily on the pre-processing results [1].

Our algorithm depends equally on both stages, enabling it to perform accurately without requiring complex pre-processing. Both the feature signal and the detection threshold are derived using the same equation, only with different window widths. We therefore demonstrate that the techniques that are often used to enhance the signal-to-noise ratio (SNR) of the QRS complex can also be used to generate an adaptable threshold that is low enough to trigger a detection for almost every QRS regardless of amplitude or morphology, yet high enough to disregard artefact and irrelevant fluctuations in the signal.

As seen in Figure 1, the algorithm supports anywhere from 1 to N leads (where N is an is an arbitrarily high number) by first performing QRS detection for each individual lead and then aggregating the leads in a weighted sum which emphasizes reliable leads and reduces the impact of noisy ones.

A. Single-lead detection

1) Pre-processing: The first step of the algorithm is a band-pass filter which enhances the QRS and reduces the P and T-waves. A fourth-order Butterworth filter with a pass-band of 7 to 17 Hz provides good detection performance and is within the prescribed range for QRS detection [1], [2]. The filtered signal $y(n)$ of sampling frequency f samples per second is then differentiated to highlight the rapid changes common in the QRS, and rectified using a simple absolute value operation to ensure that every significant peak is positive and that only one threshold is necessary for QRS detection (1). This is a standard pre-processing approach and variations of it have been used since the earliest QRS detection algorithms [2].

$$y(n) = |y(n) - y(n-1)| \tag{1}$$

2) Feature and threshold signal generation: Following pre-processing, a moving average filter is used to generate the feature signal $s_1(n)$ (2) and threshold signal $t_1(n)$ (3). The ideal feature signal window width p should be slightly larger than the average QRS width (200 milliseconds in our implementation although moderate fluctuation of any of the constants used in this algorithm does not significantly affect performance) while the threshold signal window width q should be greater than the longest RR interval or heartbeat duration expected (3 seconds in our implementation). We chose to place greater weight on the points at the centre of the window in order to increase the threshold around peaks and avoid a few false positives. In order to keep the running time of the algorithm independent of the window widths, this feature is implemented with the mean of three uniform moving averages; one with the feature signal window width, another with the threshold signal window width and a third one with a window width equal to the geometric mean of the first two (respectively 200 milliseconds, 3000 milliseconds and 775 milliseconds in our implementation).

*This work was supported by a Personnel Award from the Heart and Stroke Foundation of Canada.

The authors are with Queen's University, Kingston, Ontario, Canada.

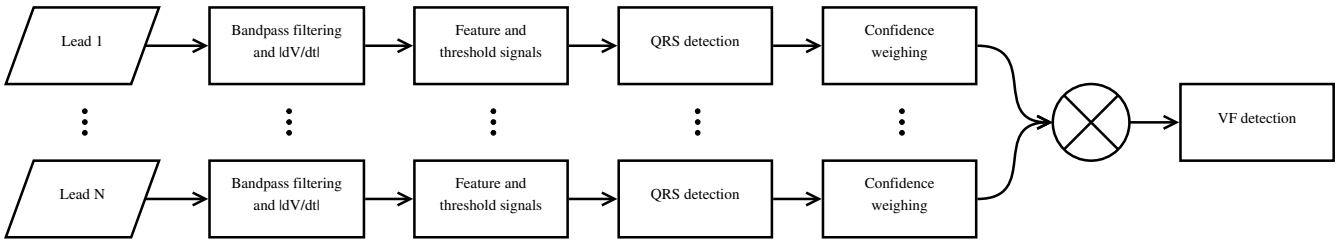

Figure 1. The various stages of our algorithm: after bandpass filtering, differentiation and rectification, the feature and threshold signals for each lead are generated from the same equation and compared to perform preliminary QRS detection. The outcome is used to assign confidence weights on the leads before they are normalized and summed to obtain the overall detection results, from which ventricular flutter and fibrillation segments are optionally identified.

$$s_1(n) = \frac{1}{p+1} \sum_{i=n-\lceil \frac{p}{2} \rceil}^{n+\lfloor \frac{p}{2} \rfloor} y(i) \tag{2}$$

$$t_1(n) = \frac{1}{3}\left[s_1(n) + \frac{\sum_{i=n-\lceil \frac{q}{2} \rceil}^{n+\lfloor \frac{q}{2} \rfloor} y(i)}{q+1} + \frac{\sum_{i=n-\lceil \frac{\sqrt{pq}}{2} \rceil}^{n+\lfloor \frac{\sqrt{pq}}{2} \rfloor} y(i)}{\lceil \frac{\sqrt{pq}}{2} \rceil + \lfloor \frac{\sqrt{pq}}{2} \rfloor + 1} \right] \tag{3}$$

3) High-amplitude-T-wave avoidance: Occasionally, T-waves can have similar amplitude and frequency characteristics as their preceding QRS complexes, resulting in false positives. They are usually avoided by not allowing the threshold to drop after a QRS detection until a refractory period of about 200 milliseconds has passed [2]. We achieve this by maintaining the threshold signal amplitude at its maximum throughout a detected QRS (which has the added advantage of avoiding merging P and T-waves to the QRS) and incorporating a decay factor $\alpha = {}^{20}/_{f}$ following the QRS in order to slow the threshold signal amplitude drop (4).

$$t_2(n) = \begin{cases} \max\limits_{i \in QRS_n} [t_1(i)] & s_1(n) > t_1(n) \\ \alpha t_1(n) + (1-\alpha) t_2(n-1) & s_1(n) \leq t_1(n) \end{cases} \tag{4}$$

B. Multi-lead detection

Once the feature and threshold signals are generated, QRS detection is simply a matter of finding the points where the feature signal amplitude is greater than the threshold signal amplitude, while merging neighbouring points (less than 50 milliseconds apart) and excluding exceptionally short detections (also less than 50 milliseconds). This entire section can be skipped if we are working with a single-lead ECG. Otherwise, performing QRS detection using multiple leads is all about resolving the differences between the leads. Our strategy consists of attaching a confidence factor to each potential QRS detection; this confidence factor is influenced by the amplitude strength of the detection as well as the likelihood of the corresponding RR interval.

1) RR interval confidence: Each RR interval is compared to the moving average of the surrounding five RR intervals. While some variability is expected, large deviations from the average could signal an incorrect detection. We minimize the impact of such incorrect detections by reducing their weight; specifically, we reduce the amplitude of the feature signal in such a way that the difference between it and the threshold signal becomes $10^{d_k} - 1$ smaller (6), where d_k is the maximum neighbouring percentage difference between the current RR interval RR_k and the moving average of the surrounding RR intervals (5). This means that if the RR interval is equal to the moving average, the feature signal is unchanged while if the RR interval is twice the moving average, the feature signal becomes ten times closer to the threshold signal (but remains on the same side of it). Note that this step does not compromise our ability to detect premature beats unless they are only seen in a minority of leads which is not usually the case. Assigning a low confidence to a detection does not mean that it is automatically excluded; it is only excluded if other leads with higher confidence values disagree with it.

$$d_k = \max_{j=k-2 \ldots k+2} \left| \frac{5 \times RR_j}{\sum_{i=j-2}^{j+2} RR_i} - 1 \right| \tag{5}$$

$$s_2(n) = \frac{s_1(n) + (10^{d_k} - 1) t_2(n)}{10^{d_k}} \tag{6}$$

2) Normalization: The next step serves the dual purpose of measuring the strength of a QRS detection and normalizing the signal in order for all leads to have the same scale. This is performed by dividing the difference between the feature and threshold signal by their sum, then smoothing using a moving average filter (7). A positive result $v(n)$ is interpreted as a QRS detection and a negative result as lack of one. The absolute value of the result represents the confidence in either decision. Figure 2 shows the algorithm stages described up to this point performed on an example signal.

$$v(n) = \frac{1}{p+1} \sum_{i=n-\lceil \frac{p}{2} \rceil}^{n+\lfloor \frac{p}{2} \rfloor} \frac{s_2(i) - t_2(i)}{s_2(i) + t_2(i)} \tag{7}$$

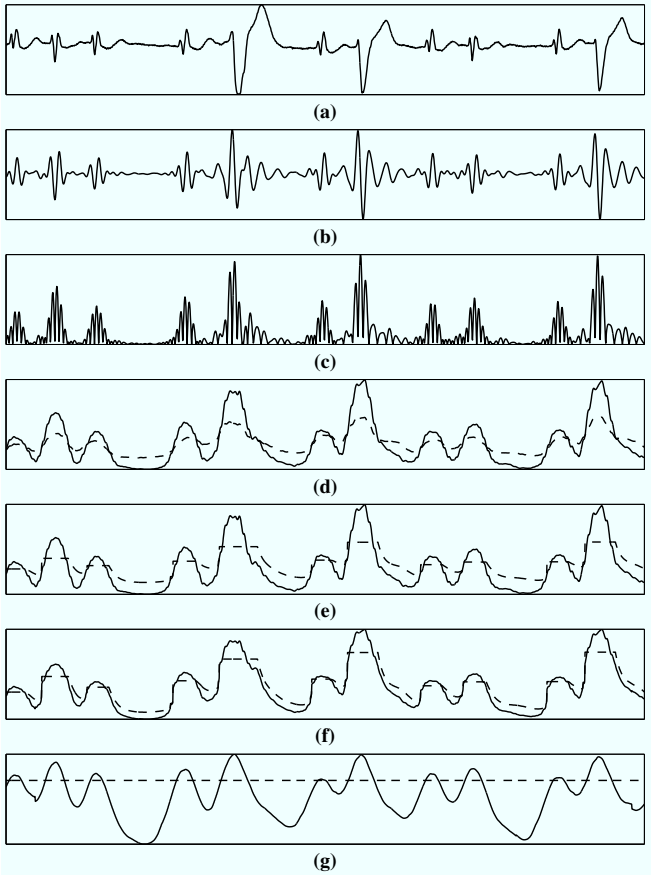

Figure 2. The various stages of our algorithm seen on the first lead of an example ECG. (a) Input signal. (b) Band-pass filtering. (c) Differentiation and rectification. (d) Solid feature signal and dashed threshold signal. (e) Threshold signal modification for T-wave avoidance. (f) RR interval confidence weighing. (g) Amplitude differerence normalization. The last two steps of the algorithm (lead combination and VF exclusion) are not shown since one would require an additional lead and the other a VF rhythm.

3) Mean of leads: Combining detections from N different leads is now simply a matter of summing their normalized results $v_i(n)$ where i is the lead number (8); scale differences among the leads are no longer an issue, and disagreements are resolved in favour of the leads with a majority of relatively confident detections. We chose to compute the mean of different leads instead of their sum in order for the scale of the result to be independent of the number of leads.

$$z(n) = \frac{1}{N}\sum_{i=1}^{N} v_i(n) \tag{8}$$

C. Ventricular flutter and fibrillation detection

Ventricular flutter and ventricular fibrillation (VF) are two heart rhythm abnormalities where the heart "quivers" instead of fully beating. As such, they lack a clear QRS complex and their corresponding ECG looks more or less like a sine wave which alternates between positive and negative peaks without a noticeable baseline. By design, our feature and threshold signals have very close amplitude throughout VF regions; this can be understood intuitively since the moving average of a sine wave is roughly constant whether we are dealing with a short or long averaging window. This results in low-confidence QRS detections during VF rhythms, which is reflected by the mean of the leads hovering around zero with a very small moving standard deviation for several beats.

We use this property to automatically and easily identify VF rhythms. This detection is essential in many cases including automated defibrillators. However, VF waves are not considered to be QRS complexes per se in standard database annotations [3] and as such they need to be excluded in order to compare our algorithm with others on an equal footing. We therefore program our algorithm to automatically identify VF and exclude it for this validation, making the two criteria for a QRS detection:

- $z(n) > 0$ at the beginning and end of an interval of at least 50 milliseconds where no two positive points are more than 50 milliseconds apart. The midpoint of that interval is selected as the QRS fiducial point.
- the moving standard deviation of $z(n)$ with a window size q should be greater than the VF threshold. Even a very low threshold (0.003 in our implementation) is capable of identifying most VF rhythms, enabling us to perform this step without significantly increasing the number of false negatives.

III. Methods

A. Database

We tested our algorithm on the MIT-BIH Arrhythmia Database [3] which is part of PhysioBank [4]. The database contains 48 half-hour two-lead ECG recordings exhibiting various arrhythmias and noise levels, and is frequently used to validate QRS detection algorithms. Parts of the database are often manually excluded from the validation of other algorithms in the literature; this could include entire recordings exhibiting high levels of noise or rhythm abnormalities, challenging portions of recordings (such as the annotated sustained VF rhythm in recording 207), or the second lead which is significantly more noisy than the first one. We chose to use the entire database as we consider this to be the most unbiased test of our algorithm.

B. Performance quantification

The performance of QRS detection algorithms is usually evaluated by the number of true positive (TP), false positive (FP), and false negative (FN) detections. We considered a detection to be a true positive if it occurred within 75 milliseconds (considerably less than the duration of an average QRS) of an annotation. Sensitivity (Se), positive predictivity (+P), and detection error rate (DER) are calculated as follows:

$$Se = \frac{TP}{TP + FN} \tag{9}$$

$$+P = \frac{TP}{TP + FP} \tag{10}$$

$$DER = \frac{FP + FN}{TP + FN} \tag{11}$$

IV. Results

Table I shows our detection performance on each of the 48 recordings of the MIT-BIH Arrhythmia Database. The algorithm achieves an overall detection error of only 0.29% with a sensitivity of 99.85% and a positive predictivity of 99.86%. To our knowledge, this exceeds the performance of any other algorithm with published results using all recordings of the same database. This can be seen in the comprehensive review by Köhler et al. [1] and more recent works presenting and referencing state-of-the-art algorithms employing diverse methods such as wavelet coefficients and multiscale mathematical morphology [5], [6], [7], [8]. It is worth noting that some of the cited algorithms require manual input to achieve their published performance; this usually involves the manual exclusion of the VF segment in recording 207 and/or the noisy second channel in all recordings.

Table I
Algorithm Performance on the MIT-BIH Arrhythmia Database

Recording	TP	FP	FN	Se (%)	+P (%)	DER (%)
100	2272	0	1	99.96	100.00	0.04
101	1864	4	1	99.95	99.79	0.27
102	2187	0	0	100.00	100.00	0.00
103	2084	0	0	100.00	100.00	0.00
104	2227	1	2	99.91	99.96	0.13
105	2555	18	17	99.34	99.30	1.36
106	2027	2	0	100.00	99.90	0.10
107	2135	0	2	99.91	100.00	0.09
108	1761	7	2	99.89	99.60	0.51
109	2532	0	0	100.00	100.00	0.00
111	2124	0	0	100.00	100.00	0.00
112	2539	0	0	100.00	100.00	0.00
113	1794	0	1	99.94	100.00	0.06
114	1879	0	0	100.00	100.00	0.00
115	1952	0	1	99.95	100.00	0.05
116	2410	0	2	99.92	100.00	0.08
117	1535	0	0	100.00	100.00	0.00
118	2278	0	0	100.00	100.00	0.00
119	1987	1	0	100.00	99.95	0.05
121	1863	0	0	100.00	100.00	0.00
122	2476	0	0	100.00	100.00	0.00
123	1518	0	0	100.00	100.00	0.00
124	1619	0	0	100.00	100.00	0.00
200	2581	3	20	99.23	99.88	0.89
201	1950	1	13	99.34	99.95	0.71
202	2133	0	3	99.86	100.00	0.14
203	2949	2	31	98.96	99.93	1.11
205	2647	0	9	99.66	100.00	0.34
207	1859	51	1	99.95	97.33	2.72
208	2921	8	34	98.85	99.73	1.42
209	3002	0	3	99.90	100.00	0.10
210	2644	1	6	99.77	99.96	0.26
212	2747	1	1	99.96	99.96	0.07
213	3249	0	2	99.94	100.00	0.06
214	2261	1	1	99.96	99.96	0.09
215	3362	0	1	99.97	100.00	0.03
217	2208	0	0	100.00	100.00	0.00
219	2154	1	0	100.00	99.95	0.05
220	2047	0	1	99.95	100.00	0.05
221	2427	0	0	100.00	100.00	0.00
222	2482	1	1	99.96	99.96	0.08
223	2603	0	2	99.92	100.00	0.08
228	2053	0	0	100.00	100.00	0.00
230	2256	0	0	100.00	100.00	0.00
231	1571	14	0	100.00	99.12	0.88
232	1780	31	0	100.00	98.29	1.71
233	3071	0	8	99.74	100.00	0.26
234	2753	0	0	100.00	100.00	0.00
Total	**109328**	**148**	**166**	**99.85**	**99.86**	**0.29**

V. Discussion

A. Time complexity

The algorithm's running time is linear in the length (number of samples) of the input signal, which makes it ideal for embedded and low-power applications such as mobile and implantable devices. Practically speaking, a MATLAB (Version R2010b, The MathWorks Inc., Natick, MA, 2010) implementation running on our entry-level dual-core computer analyzes each half-hour recording in less than five seconds.

B. Multi-lead detection

Our algorithm does not depend on any particular lead configuration; as such, is does not need to know in advance the number of leads, their positions, or their relative noise levels. Instead, it considers all input leads and has the ability to automatically boost relevant leads and reduce the impact of noisy ones. This minimizes human input and makes it a very versatile algorithm useful for multiple applications from 12-lead hospital electrocardiograms to ambulatory long-term recording and exercise testing where lead numbers and positions can vary and detached leads are not uncommon.

References

[1] B. Köhler, C. Hennig, and R. Orglmeister, "The principles of software QRS detection," *IEEE Engineering in Medicine and Biology Magazine: The Quarterly Magazine of the Engineering in Medicine & Biology Society*, vol. 21, no. 1, pp. 42–57, Feb. 2002, PMID: 11935987. [Online]. Available: http://www.ncbi.nlm.nih.gov.proxy.queensu.ca/pubmed/11935987

[2] J. Pan and W. J. Tompkins, "A Real-Time QRS detection algorithm," *IEEE Transactions on Biomedical Engineering*, vol. BME-32, no. 3, pp. 230–236, Mar. 1985.

[3] G. B. Moody and R. G. Mark, "The impact of the MIT-BIH arrhythmia database," *IEEE Engineering in Medicine and Biology Magazine: The Quarterly Magazine of the Engineering in Medicine & Biology Society*, vol. 20, no. 3, pp. 45–50, Jun. 2001, PMID: 11446209. [Online]. Available: http://www.ncbi.nlm.nih.gov/pubmed/11446209

[4] A. L. Goldberger, L. A. N. Amaral, L. Glass, J. M. Hausdorff, P. C. Ivanov, R. G. Mark, J. E. Mietus, G. B. Moody, C. Peng, and H. E. Stanley, "PhysioBank, PhysioToolkit, and PhysioNet : Components of a new research resource for complex physiologic signals," *Circulation*, vol. 101, no. 23, pp. e215–e220, Jun. 2000. [Online]. Available: http://circ.ahajournals.org/content/101/23/e215

[5] M. Adnane, Z. Jiang, and S. Choi, "Development of QRS detection algorithm designed for wearable cardiorespiratory system," *Computer Methods and Programs in Biomedicine*, vol. 93, no. 1, pp. 20–31, Jan. 2009. [Online]. Available: http://www.sciencedirect.com/science/article/pii/S0169260708001879

[6] F. Zhang and Y. Lian, "QRS detection based on multiscale mathematical morphology for wearable ECG devices in body area networks," *IEEE Transactions on Biomedical Circuits and Systems*, vol. 3, no. 4, pp. 220–228, Aug. 2009.

[7] Y. Wang, C. J. Deepu, and Y. Lian, "A computationally efficient QRS detection algorithm for wearable ECG sensors," in *2011 Annual International Conference of the IEEE Engineering in Medicine and Biology Society,EMBC*. IEEE, Sep. 2011, pp. 5641–5644.

[8] Z. Zidelmal, A. Amirou, M. Adnane, and A. Belouchrani, "QRS detection based on wavelet coefficients," *Computer Methods and Programs in Biomedicine*, Jan. 2012. [Online]. Available: http://linkinghub.elsevier.com/retrieve/pii/S016926071100321X